A cross-scale view of N and P limitation using a Bayesian hierarchical model

YoonKyung Cha [a], Ibrahim Alameddine [b*], Song S. Qian [c], Craig A. Stow [d]

[a] School of Environmental Engineering, University of Seoul, Seoul, South Korea, ykcha@uos.ac.kr

[b] Department of Civil and Environmental Engineering, American University of Beirut, Beirut, Lebanon, ia04@aub.edu.lb

[c] Department of Environmental Sciences, The University of Toledo, Toledo, OH 43606, USA, song.qian@utoledo.edu

[d] NOAA Great Lakes Environmental Research Laboratory, Ann Arbor, MI, 48108, USA, craig.stow@noaa.gov

[*] Corresponding author. Tel +9611350000; Email address: ia04@aub.edu.lb

Keywords: N:P ratio, Bayesian, hierarchical model, Finnish lakes, Saginaw Bay, Neuse Estuary, and eutrophication management

Abstract

We propose a bivariate Bayesian hierarchical model (BBHM), which adds a perspective on a century-long subject of research, nitrogen (N) and phosphorus (P) dynamics in freshwater and coastal marine ecosystems. The BBHM is differentiated from existing approaches by modeling multiple aspects of N-P relationships—N and P concentration variability, ratio, and correlation—simultaneously, allowing these aspects to vary by seasonal and/or spatial components. The BBHM is applied to three aquatic systems, Finnish Lakes, Saginaw Bay, and the Neuse Estuary, which exhibit differing landscapes and complexity of nutrient dynamics. Our model reveals N and P dynamics that are critical to inferring unknown N and P distributions for the overall system as well as for within system variability. For Finnish lakes, strong positive within- and among-lake N and P correlations indicate that the rates of N and P biogeochemical cycles are closely coupled during summer across the different lake categories. In contrast, seasonal decoupling between N and P cycles in Saginaw Bay is evidenced by the large variability in monthly correlations and the seasonal changes in the N distribution. The results underscore the pivotal role that dreissenids have had on the cycling of nutrients and resurgence of eutrophication. The presence of clear seasonality and a spatial gradient in the distributions and N and P in the Neuse Estuary suggest that riverine N input is an important source in the season-space N dynamics, while summer sediment release is a major process regulating seasonal P distribution.

Introduction

Eutrophication mitigation is an ongoing challenge in aquatic ecosystem management. Reducing nutrient inputs remains the most viable option for eutrophication control, and management actions are generally directed toward controlling the nutrient, either nitrogen (N) or phosphorus (P), that is believed to limit primary production. The prevailing outlook since the 1970s has been that P is generally limiting in freshwater systems, while N usually limits algal growth in coastal, marine environments (Krumbein, 1981; Lee and Olsen, 1985; Carpenter et al. 1998; Howarth and Marino 2006, Steward and Lowe, 2010). Redfield (1958) established that the atomic ratio of N:P in oceanic phytoplankton was ~16:1 (7.2:1 mass ratio) and this value is regarded as an approximate threshold delineating N vs. P limitation in both marine and freshwater systems (Guildford and Hecky 2000). Above the Redfield ratio, a system is usually considered P limited, while below this threshold N is likely to be limiting, assuming that some other characteristic is not restricting algal production. While the Redfield ratio does not fully characterize, with high certainty, nutrient limitation across all aquatic systems, it remains an easy to quantify metric that is commonly consulted in the development of eutrophication management plans.

The strict view of P vs. N limitation is currently being reexamined (Lewis and Wurtsbaugh 2008), with arguments that joint nutrient control is appropriate for managing eutrophication in coastal, marine and inland systems (Howarth and Marino 2006; Paerl 2009; Lewis et al. 2011). These assertions have arisen as localized seasonal N limitation has been documented in Lake Erie (Chaffin et al. 2013; Chaffin et al. 2014), a freshwater system long regarded as P limited. Observations of P limitation in tropical estuaries and coastal areas (Smith, 1984; Short et al. 1990) and the seasonal switching of limitation in several temperate estuaries (Myers and Iverson; 1981, Nowicki and Nixon, 1985; Malone et al. 1996; Rabalais et al. 2002; Cugier et al. 2005) have also highlighted the importance of P in controlling growth in brackish/saltwater systems. Additionally, N and P co-limitation has frequently been indicated in small scale experiments (Sterner, 2008). Moreover, the role of N and P stoichiometry in algal toxin production has recently come under investigation (Cugier et al. 2005; Smith and Schindler 2009; Davis et al. 2010; Van de Waal et al. 2014; Yuan et al. 2014).

While it is widely recognized that N and P concentrations and the N:P ratio can differ at various spatiotemporal scales (Downing 1997; Fisher et al. 1999; Hall et al. 2005), it is common to characterize systems using point estimates or summary statistics that integrate N and P spatially and/or temporally. Scale-aggregated measures may hide important system dynamics that influence N and P, and consequently, phytoplankton productivity. Additionally, because many processes affect both N and P, their concentrations are often correlated, and evaluating them independently may be misleading. Tracking changes in the correlation structure can reveal coupling and decoupling between N and P, and provide clues about the biogeochemical processes underlying these patterns.

To reveal the differing spatiotemporal dynamics of N and P within and among systems, we adopt a Bayesian hierarchical modeling approach that jointly characterizes N and P concentrations at multiple scales simultaneously, while accounting for spatio-temporal changes in their correlations. For examples we use three well-studied aquatic systems, lakes in Finland, Saginaw Bay-Michigan, USA, and the Neuse River Estuary-North Carolina, USA, each of which are aggregated at different spatial and temporal scales, and exhibit differing patterns and processes that regulate N and P behavior.

Methods

Study sites and data description

For Finnish lakes, total N (TN) and total P (TP) concentrations were sampled from 2,289 lakes during the summer (July and August) from 1988 to 2004 (Table 1 and Figure 1) (Malve and Qian 2006). Samples are unevenly distributed among years, types, and lakes; on average eight water quality samples were collected from each lake. Finnish lakes are classified by the Finnish Environment Institute (SYKE) into nine types based on expert assessments on lake morphology and chemistry, such as depth, surface area, and color (Table 2). According to SYKE, the selected types describe the ecological status of the lakes within each group.

Saginaw Bay is a large embayment (~2,700 km^2) on Lake Huron, located in Michigan, USA (Figure 1). Our analysis focuses on the inner portion of the Bay, which can be characterized as shallow (mean depth ~5 m), warm, and eutrophic (Stow et al. 2014). TN and TP data for the bay during the growing season (April to November) of 1999-2007 were obtained from the United States Environmental Protection Agency's online STORET database (Table 1). We used Saginaw Bay as an example to highlight the seasonality of nutrient dynamics and how the N and P behavior can provide evidence on the presence of a latent variable that is mediating these changes.

The Neuse River Estuary, on the coast of North Carolina, USA, has been described in many previous reports (Mallin et al. 1993; Borsuk et al. 2004; Alameddine et al. 2011). The estuary is shallow with a mean depth of 3.6 m, a mean width of 6.5 km, a total length of 70 km, and experiences a gradient of conditions along its length (Arhonditsis et al. 2007). The uppermost section is freshwater-dominated, with high nutrient concentrations. Nutrient concentrations tend to decrease and salinity levels increase further downstream. We examined dissolved inorganic N (DIN) and dissolved inorganic P (DIP) concentrations collected from 2000 - 2005 obtained from the ModMon program (http://www.unc.edu/ims/neuse/modmon) (Table 1). These data were collected every other week in all seasons at five sections across the riverine-estuarine parts of the system (Figure 1). The division of the estuary into five sections captures the nutrient and salinity gradient within the estuary (Wool et al., 2003; Borsuk, et al. 2004; Lebo et al. 2012). Data for the Neuse were grouped temporally by season, and aggregated spatially into five segments along the freshwater-salinity gradient.

Model Development

We developed a bivariate Bayesian hierarchical model (BBHM) to highlight changes in the N:P relationship within and across scales by quantifying the variability in the concentration, ratio and correlation of N and P both at fine spatiotemporal scales (within a season or month, or within specific sections of a system) and at coarser scales (over multiple years, or across geographic regions). Bayesian hierarchical models are naturally suited for analyzing data from multiple units that are related and exhibit cross-scale structure (Qian et al. 2010; Soranno et al. 2014). They are also advantageous for estimating multiple group means, e.g., seasonal or spatial means of N and P concentrations, because they benefit from the effect of shrinking group mean estimates toward the overall mean when data are either sparse or show high variability (Qian et al. 2015). The BBHM contrasts with traditional N:P point estimates that tend to ignore the spatiotemporal correlations among sites and/or seasons, thus implicitly assuming that data from different sites/months are independent of each other. Evidence of increased estimation accuracy by pooling data from similar variables (e.g., nutrient concentrations from multiple sites) has emerged as early as the 1950s (Stein, 1955). Like most water quality concentration variables, N and P concentrations are right-skewed and bounded at zero. Their univariate distributions are often approximated by a lognormal distribution (Ott 1995). We used a bivariate normal distribution to model log-transformed N and P concentrations and their correlation. N and P concentrations were simultaneously modeled at two different levels. At the individual measurement level, covarying N and P distributions were estimated for each defined group:

$$log(X_{ij}) \sim BVN(\theta_j, \Sigma_j) \quad (1)$$

The group level N and P concentrations were then linked to an overall system level N and P distribution:

$$\theta_j \sim BVN(\mu, T) \quad (2)$$

for $\Sigma_j = \begin{pmatrix} \sigma_{N_j}^2 & \rho_j \sigma_{N_j} \sigma_{P_j} \\ \rho_j \sigma_{N_j} \sigma_{P_j} & \sigma_{P_j}^2 \end{pmatrix}$,

and $T = \begin{pmatrix} \tau_N^2 & \varphi \tau_N \tau_P \\ \varphi \tau_N \tau_P & \tau_P^2 \end{pmatrix}$,

where the subscript i represents an observation and j represents a group (j=1,…,9 for the Finnish Lakes example, representing lake types; j=1,…,8 for the Saginaw Bay example, representing months; j=1,…,20 for the Neuse River Estuary example, representing the combination of 4 seasons and 5 sections of the estuary), $X_{ij} = \begin{bmatrix} X_{N_{i,j}} \\ X_{P_{i,j}} \end{bmatrix}$ is the vector of N and P concentration measurements at sample i and group j. BVN indicates the bivariate normal distribution with the mean vector, $\theta = \begin{bmatrix} \theta_N \\ \theta_P \end{bmatrix}$, and the covariance matrix, Σ. The group mean vectors were linked by a system-level bivariate normal distribution with mean vector, $\mu = \begin{bmatrix} \mu_N \\ \mu_P \end{bmatrix}$, and covariance matrix, T. In the covariance matrices σ and τ are standard deviations, and ρ and φ are correlation coefficients. The model is a natural representation of the data structure that permits accounting for the full correlations in the data. The likelihood function of a given sample X_{ij} is thus:

$$L(\theta, \Sigma) = \frac{1}{(2\pi)^{0.5nk} |\Sigma|^{0.5n}} e^{\left(-\frac{1}{2}\sum_{i=1}^{n}(X-\theta)^T \Sigma^{-1} (X-\theta)\right)} \quad (3)$$

$$\propto \frac{1}{|\Sigma|^{0.5n}} e^{\left(-\frac{1}{2}tr(S\Sigma^{-1})+n(\theta-\bar{X})^T\Sigma^{-1}(\theta-\bar{X})\right)}$$

where $\bar{X} = \frac{1}{n}\sum_{i=0}^{n} X_i$ and $S = \sum_{i=1}^{n}(X_i - \bar{X})(X_i - \bar{X})^T$ and tr is the trace of the matrix. Under a Bayesian framework, prior distributions need to be specified for the model parameters, δ = (ρ_j, $\sigma_{N,j}$, $\sigma_{P,j}$), as well as the model's hyperparameters, Δ = (μ_N, μ_P, φ, τ_N, τ_P). We used diffuse priors on all model parameters and hyperparameters (Table 3). A Markov chain Monte Carlo simulation method implemented in the software program WinBUGS 1.4.3 (Lunn et al 2000) was used to simulate random samples of all model parameters from their joint posterior distributions. A model run was considered to have converged when the potential scale reduction parameter ($\hat{R}$) for all parameters was one (Gelman and Rubin, 1992; Gelman and Hill 2007). Model goodness-of-fit was evaluated at the observational level by using the pivotal discrepancy measure (PDM) proposed by Yuan and Johnson (2012). The WinBUGS code for the three systems is included in the online supplementary information.

N:P ratio distributions were derived from posterior samples of N and P at appropriate scales. For example, log within-group ratios were estimated by ($\theta^m{}_{N,j} - \theta^m{}_{P,j}$) and log system-wide ratio was estimated by ($\mu^m{}_N - \mu^m{}_P$), where *m* represents the *m*th MCMC sample from the joint posterior distribution of all parameters. The adopted model structure reflects dependencies both between individual measurements and their corresponding group as well as across the groups and the system as a whole.

Results

Individual N and P observations were positively correlated in the Finnish Lakes and Saginaw Bay (sample correlation coefficients r = 0.62 and 0.41, respectively) while there was little correlation in the Neuse Estuary (r = 0.05) at this scale (Figure 2a, b, c). Observations in the Finnish lakes are generally above the Redfield ratio as are the median values for each lake group (Figure 2a). In Saginaw Bay all observations and monthly medians exceed the Redfield ratio (Figure 2b). In contrast, observations and group medians straddle the Redfield ratio in the Neuse (Figure 2c).

N:P ratios (estimated by $e^{\theta_N}: e^{\theta_P}$) show differing within group structure for each of the study sites (Figure 2d, e, f). The Finnish lakes exhibit a consistent strong positive correlation between N and P within each group (Figure 3a). All groups are well above the Redfield ratio (Figures 2d and 4a), with ratios ranging from 17:1 to > 30:1 across lake types (Figure 4a). Consistent with the within lake-type N and P correlation, the Finnish lake system as a whole shows a strong positive correlation that approached one. In contrast, while the within-group correlations are all positive in Saginaw Bay, the strength of correlation differs seasonally (Figure 3b); correlations are strongest in the spring and early summer and weaken over the summer. N:P ratios are also observed to progress toward the Redfield ratio as summer progresses (Figures 2e and 4b).

The Neuse, which was grouped spatially and temporally, exhibits a more complex pattern than the other two sites. The Neuse exhibited more differentiation in the N:P correlation. For each of the five estuarine segments, it was highest in the spring, with a decline through summer and fall, followed by a rise in the winter (Figure 3c). Groups in the Neuse spanned the Redfield ratio (Figure 2f), the N:P ratio generally decreased moving from upstream to downstream and from fresher to more saline conditions (Figures 2f and 4c).Yet, across all locations there was a general seasonal progression in N:P ratios. Highest ratios were observed in winter and spring, lower ratios were found in the summer, after which the ratio subsequently increased in the fall (Figures 2f and 4c). Interestingly, both ratios and correlations followed the same temporal pattern.

System-wide N:P ratios (estimated by $e^{\mu_N}: e^{\mu_P}$) summarize overall across-group structure (Figure 2g, h, i). The N:P correlation across groups (φ) in the Finnish lakes was found to be strongly positive (very close to one) (Figure 2g; Figure 3a). Moreover, the overall N:P ratio for the entire system of lakes was well above the Redfield ratio (Figure 2g). The temporally based grouping in Saginaw Bay showed a negative across-months N:P correlation (Figures 2h and 3b), but overall the Bay was above the Redfield ratio (Figure 2h). In the Neuse, across group correlation was positive (Figures 2i and 3c) and overall the system was below the Redfield ratio, though the system as a whole had a small probability of exceeding it (Figure 2i).

Discussion

Our results illustrate the utility of the BBHM to reveal N and P patterns that are not well captured by point estimates and summary statistics. This is accomplished by accounting for the covarying nature of N and P along with their variability over the time-space scales of interest. The model enables us to summarize the wide observed range of water column N and P concentrations and ratios (Figure 2), as well as characterize their spatio-temporal variation.

The model captures multiple aspects of the N-P relationship—N and P concentration variability and correlation—simultaneously, through which N:P ratio distribution can also be characterized. Putting all the pieces together is important in assessing N and P dynamics because both the ratios and concentrations are indicative of trophic state and influence algal biomass and community composition (Smith 1982; Hecky and Kilham 1998; Smith and Bennett 1999; Guildford and Hecky 2000; Howarth and Marino 2005).

The correlation between N and P concentrations has seldom come to the forefront, in contrast to the ratio, despite the fact that the correlation carries a signal of coupling between N and P cycles along the time of year through space. Strong, positive within- and across-group correlations for the Finnish lakes (Figure 4a) may indicate that the rates of N and P biogeochemical cycles in the summer are similar to each other both by lake-type and at the whole system-scale, albeit with different levels of P limitations. This strong coupling may mislead nutrient management decisions aiming to reduce eutrophication, particularly when N:P ratios are not consulted. The spatial distribution of N and P in Finnish lakes suggests that lake color, an indicator of dissolved carbon and humic acids, appears to be a better predictor of trophic state as compared to lake size or depth. Humic lakes appear to consistently have higher nutrient concentrations and lower N:P ratios as compared to non-humic lakes, irrespective of area and/or depth. Color levels tended to be related with N and P levels (Table 2, Figure 2d). These relationships among the color, N and P levels were confirmed in 600 freshwater lake systems (Nürnberg and Shaw, 1998).

In Saginaw Bay, a negative across-month correlation was found, which contrasts with the positive correlations observed within each month (Figure 4b). This apparent inconsistency is an illustration of Simpson's paradox (Simpson, 1951) that arises from partitioning data into subpopulations. This apparent inconsistency suggests differing drivers at shorter vs. longer time-scales. The negative across-month pattern arises as monthly P concentrations generally increase from spring through fall, while monthly N concentrations generally decrease (Figure 3e). Interestingly, data from 1974 indicated spring peaks for both P and N concentrations (Bierman and Dolan 1981), and Stow et al (2014) reported an apparent shift in the phosphorus peak following the early 1990s dreissenid mussel invasion. The negative correlation across months may reveal a decoupling of the seasonal N and P concentration drivers which results from differing mussel filtration rates through the year. Spring tributary inputs likely consist of a high proportion of dissolved N, which is not removed via mussel filtration, and a high proportion of particulate P, which is removed by the mussels. As N and P tributary inputs decrease into the summer, so does the mussel filtration rate (Nalepa and Fahnenstiel 1995, Vanderploeg et al 2009), favoring a relative increase in P concentrations in the bay, while N concentrations respond primarily to the declining tributary load. Thus, while tributary inputs are a common driver for N and P, at longer time-scales differential internal processing causes divergent behavior in their concentrations. Failing to understand or resolve the paradoxical association between N and P at different scales can often lead to unsuitable nutrient management plans.

The Neuse River Estuary exhibits a wide variation in within-group N:P correlation (Figure 3c). The correlation is highest in the spring and at the upstream stations, probably reflecting spring precipitation and associated watershed inputs as the main driver of N and P concentrations. Moving downstream, and during lower flow conditions, internal processes, which differentially influence N and P concentrations appear to dominate resulting in a decoupling of N and P. N concentrations in the Neuse Estuary exhibit clear spatial gradients and distinguishable seasonality (Figure 3c). High winter-spring N concentrations followed by low summer-fall N, combined with the high upstream to low estuarine N gradient, suggest that riverine input, over internal processing, is a dominant factor in season-space N dynamics in the estuary. Like most temperate estuaries, the lower saline sections of the Neuse Estuary show strong nitrogen limitations, highlighting the importance of oceanic inputs and the lack of significant planktonic N fixation (Howarth 1998; Vitousek and Howarth 1991; Nixon et al. 1995; Howarth and Marino 2005). Conversely, summer P peaks may imply that sediment release associated with bottom-water anoxia is an important process influencing water column P concentrations during summer (Paerl et al. 1998; Alameddine at al. 2011).

Although the Finnish lakes, Saginaw Bay, and the Neuse River Estuary reveal a mesotrophic state at the system scale (Figure 2), variability of N and P concentrations among season or space was substantial (Figure 3), as was the variability of the N:P ratios (Figure 4). Given environmental heterogeneity and uncertainty, nutrient limitation of primary producers should not be determined by any single N:P ratio. Rather, N:P ratios characterize imbalances between N and P, and noticeable deviation from the Redfield ratio may be indicative of a high likelihood of N or P nutrient limitation (Hecky and Kilham 1988). Moreover, spatio-temporal shifts in the N:P ratios are often a sign of a decoupling in the nutrient cycles. In Saginaw Bay, monthly N:P ratios were all higher than the Redfield ratio, despite clear seasonality, exhibiting a tendency of continuing P limitation throughout the growing season (Figure 2e, 4b). In the Neuse Estuary, on the other hand, complex season-space N:P patterns indicate a shifting limitation between N and P with changes in season and space (Figure 2f, 4c).

The future application of the BBHM to other aquatic systems, which are also likely to exhibit systematic spatiotemporal differences in N and P concentrations and ratios, will enable us to characterize the nutrient limitation shift linked to specific conditions or points along a continuum of time and space. The model results highlight the need for future management-oriented load-response eutrophication models to embrace a cross-scale view of nutrient limitation. Thus, future research should link this model to biological components, such as phytoplankton abundance, or toxin concentrations, so that relevant eutrophication ecosystem response indicators are probabilistically predicted as a function of covarying N and P, while also accounting for temporal and spatial dimensions.

The fundamental eutrophication management question of whether to use single or dual nutrient control strategies is the subject of much debate in the environmental and ecological science community. Our results, suggest that differing perspectives on this question may arise depending on the scale at which the system is viewed. N and P distributions on an entire system-scale distinct from those on a group-scale necessitate the science and management community to consider the mechanisms that affect eutrophication patterns on the scale of interest. Atmospheric deposition, climate and watershed characteristics such as land-use should be accentuated on the system-scale, whereas the role of riverine nutrient input and internal processes such as sedimentation, recycling, grazing or nitrification-denitrification may be critical in determining seasonal or spatial variability in N and P dynamics.

Acknowledgments

The authors thank Dr. Hans Paerl at the Institute of Marine Sciences, University of North Carolina at Chapel Hill and Dr. Olli Malve at the Finnish Environment Institute for providing the data for the Neuse River Estuary and the Finnish lakes respectively. This work was supported by NOAA's Great Lakes Environmental Research Laboratory (NOAA GLERL contribution number 1823).

References

Alameddine, I., S. S. Qian, and K. H. Reckhow. 2011. A Bayesian changepoint-threshold model to examine the effect of TMDL implementation on the flow-nitrogen concentration relationship in the Neuse River basin. Water Res **45:** 51-62.

Arhonditsis, G. B., C. A. Stow, H. W. Paerl, L. M. Valdes-Weaver, L. J. Steinberg, and K. H. Reckhow. 2007. Delineation of the role of nutrient dynamics and hydrologic forcing on phytoplankton patterns along a freshwater-marine continuum. Ecol Model **208:** 230-246.

Bierman, V. J., and D. M. Dolan. 1981. Modeling of phytoplankton-nutrient dynamics in Saginaw Bay, Lake Huron. J Great Lakes Res **7:** 409-439.

Borsuk, M.E., C.A. Stow, and K.H. Reckhow. 2004. Confounding effect of flow on estuarine response to nitrogen loading. J Environ Eng-ASCE **130**(6), 605-614.

Carpenter, S. R., N. F. Caraco, D. L. Correll, R. W. Howarth, A. N. Sharpley, and V. H. Smith. 1998. Nonpoint pollution of surface waters with phosphorus and nitrogen. Ecol Appl **8:** 559-568.

Chaffin, J. D., T. B. Bridgeman, and D. L. Bade. 2013. Nitrogen constrains the growth of late summer cyanobacterial blooms in Lake Erie. Adv Microbiol **3:** 16-26.

Chaffin, J. D., and T. B. Bridgeman. 2014. Organic and inorganic nitrogen utilization by nitrogen-stressed cyanobacteria during bloom conditions. J Appl Phycol **26:** 299-309.

Cugier, P.G. Billen, J.E Guilland, J. Garnier, and A. Mtinesguen. 2005. Modelling the eutrophication of the Seine Bight (France) under historical, present and future riverine nutrient loading. J. Hydrol. **304**: 381-396.

Davis, T. W. and others 2010. Effects of nitrogenous compounds and phosphorus on the growth of toxic and non-toxic strains of Microcystis during cyanobacterial blooms. Aquat Microb Ecol **61:** 149-162.

Downing, J. A. 1997. Marine nitrogen: Phosphorus stoichiometry and the global N:P cycle. Biogeochemistry **37:** 237-252.

Fisher, T. R. and others 1999. Spatial and temporal variation of resource limitation in Chesapeake Bay. Mar Bio **133:** 763-778.

Gelman, A. and D.B. Rubin, 1992. Inference from iterative simulation using multiple sequences. In: Gelman, A. and Hill, J. [eds]. Data Analysis using Regression and Multilevel/Hierarchical Models. Cambridge University Press, New York.

Gelman, A. and J. Hill. 2007. Data analysis using regression and multilevel hierarchical models. Cambridge: Cambridge University Press.

Guildford, S. J. and R. E. Hecky. 2000. Total nitrogen, total phosphorus, and nutrient limitation in lakes and oceans: Is there a common relationship? Limnol Oceanogr **45:** 1213-1223.

Hall, S. R., V. H. Smith, D. A. Lytle, and M. A. Leibold. 2005. Constraints on primary producer N : P stoichiometry along N : P supply ratio gradients. Ecology **86:** 1894-1904.

Hecky, R. E., and P. Kilham. 1988. Nutrient Limitation of Phytoplankton in Fresh-Water and Marine Environments - a Review of Recent-Evidence on the Effects of Enrichment. Limnol Oceanogr **33:** 796-822.

Howarth, R.W. 1988. Nutrient limitation of net primary production in marine ecosystems. Ann Rev Ecol Syst **19**: 89-110.

Howarth, R. W. and R. Marino. 2006. Nitrogen as the limiting nutrient for eutrophication in coastal marine ecosystems: Evolving views over three decades. Limnol Oceanogr **51:** 364-376.

Krumbein, W.E. 1981. Biogeochemical and geomicrobiological of lagoons and lagoonary environments. In: UNESCO Coastal Lagoon Research: Present and Future. Beaufort, N.C. August 1978. UNESCO. Technical paper in Marine Science **33**, 97-110.

Lebo, M.E., H.W. Paerl, and B.L. Peierls. 2012. Evaluation of progress in achieving TMDL mandated nitrogen reductions in the Neuse River Basin, North Carolina. Environ Manage **49**(1), 253-266.

Lee, V. and S. Olsen. 1985. Eutrophication and management initiatives for the control of nutrient inputs to Rhode Island coastal lagoons. Estuaries **8**(2B): 191-202.

Lewis, W. M. and W. A. Wurtsbaugh. 2008. Control of Lacustrine Phytoplankton by Nutrients: Erosion of the Phosphorus Paradigm. Int Rev Hydrobiol **93:** 446-465.

Lewis, W. M., W. A. Wurtsbaugh, and H. W. Paerl. 2011. Rationale for Control of Anthropogenic Nitrogen and Phosphorus to Reduce Eutrophication of Inland Waters. Environ Sci Technol **45:** 10300-10305.

Lunn, D. J., A. Thomas, N. Best, and D. Spiegelhalter. 2000. WinBUGS - A Bayesian modelling framework: Concepts, structure, and extensibility. Stat Comput **10:** 325-337.

Mallin, M. A., H. W. Paerl, J. Rudek, and P. W. Bates. 1993. Regulation of Estuarine Primary Production by Watershed Rainfall and River Flow. Mar Ecol-Prog Ser **93:** 199-203.

Malone, T.C., D.J. Conley, T.E Fisher, P.M. Glibert, L.W. Harding, and K.G. Sellner.1996. Scales of nutrient-limited phytoplankton productivity in Chesapeake Bay. Estuaries, **19**: 371-385.

Malve, O., and S. S. Qian. 2006. Estimating nutrients and chlorophyll a relationships in Finnish lakes. Environ Sci Technol **40:** 7848-7853.

Meyers, V. B. and R.I. Iverson. 1981. Phosphorus and nitrogen limited phytoplankton productivity in Northeastern Gulf of Mexico coastal estuaries. In: B.J. Neilson and L.E. Cronin [eds]. Estuaries and nutrients. Humana. 569-582.

Nalepa, T. F. and G. L. Fahnenstiel. 1995. Preface - Dreissena palymorpha in the Saginaw Bay, Lake Huron ecosystem: Overview and perspective. J Great Lakes Res **21:** 411-416.

Nixon, S.W. 1995. Coastal marine eutrophication: a definition, social causes, and future concerns. Ophelia 41: 199-219.

Nowicki, B.L. and S.W. Nixon. 1985. Benthic nutrient remineralization in a coastal lagoon ecosystem. Estuaries, **8**(2), 182-190.

Nürnberg, G. K. and M. Shaw. 1998. Productivity of clear and humic lakes: nutrients, phytoplankton, bacteria. Hydrobiologia, **382**:(1-3), 97-112.

Ott, W. R. 1995. Environmental statistics and data analysis. CRC Press L.L.C, Boca Raton.

Paerl, H. W. 2009. Controlling Eutrophication along the Freshwater-Marine Continuum: Dual Nutrient (N and P) Reductions are Essential. Estuar Coast **32:** 593-601.

Paerl, H. W., J. L. Pinckney, J. M. Fear, and B. L. Peierls. 1998. Ecosystem responses to internal and watershed organic matter loading: consequences for hypoxia in the eutrophying Neuse river estuary, North Carolina, USA. Mar Ecol-Prog Ser **166:** 17-25.

Qian, S.S. 2014. Ecological threshold and environmental management: a note on statistical methods for detecting thresholds. Ecol Indic **38**: 192-197.

Qian, S. S., C. A. Stow, and Y. Cha. 2015. Implications of Stein's Paradox for Environmental Standard Compliance Assessment. Environ Sci Technol **49:** 5913-5920.

Qian, S. S., T. F. Cuffney, I. Alameddine, G. Mcmahon, and K. H. Reckhow. 2010. On the application of multilevel modeling in environmental and ecological studies. Ecology **91:** 355-361.

Rabalais, N.N., R.E., Turner, Q., Dortch, D., Justic, V.J., Bierman, and W.J. Wiseman. (2002). Nutrient-enhanced productivity in the northern Gulf of Mexico: past, present and future. Hydrobiologia, **475**(1), 39-63.

Redfield, A. C. 1958. The biological control of chemical factors in the environment. Am Sci **46:** 205-221.

Short, F.T., W.C. Dennison, and D.C. Capone. 1990. Phosphorus-limited growth of the tropical seagrass *Syringodium filiforme* in carbonate sediments. Mar Ecol Prog. **62**: 169-174.

Simpson, E. H. 1951, The interpretation of interaction in contingency tables, J R Stat Soc Ser B, **13**(2), 238–241.

Smith, V. H. 1982. The Nitrogen and Phosphorus Dependence of Algal Biomass in Lakes - an Empirical and Theoretical-Analysis. Limnol Oceanogr **27:** 1101-1112.

Smith, V. H. 1984. Phosphorus vs nitrogen limitation in the marine environment. Limnol Oceanogr **29**: 1149-1160.

Smith, V. H., and S. J. Bennett. 1999. Nitrogen : phosphorus supply ratios and phytoplankton community structure in lakes. Arch Hydrobiol **146**: 37-53.

Smith, V. H. and D.W. Schindler. 2009. Eutrophication science: where do we go from here? Trends Ecol Evol **24**(4): 201-207.

Soranno, P. A. and others 2014. Cross-scale interactions: quantifying multiscaled cause-effect relationships in macrosystems. Front Ecol Environ **12:** 65-73.

Stein, C. 1955. Inadmissibility of the usual estimator for the mean of a multivariate normal distribution. In: Proceedings of the Third Berkeley symposium on mathematical statistics and probability. **1**(399); 197-206.

Sterner, R. W. 2008. On the Phosphorus Limitation Paradigm for Lakes. Int Rev Hydrobiol **93:** 433-445.

Stewards, J.S., and E.F. Lowe. 2010. General empirical models for estimating nutrient load limits for Florida's estuaries and inland waters. Limnol Oceanogr **55**(1): 433-445.

Stow, C. A. and others 2014. Phosphorus targets and eutrophication objectives in Saginaw Bay: A 35 year assessment. J Great Lakes Res **40:** 4-10.

Van De Waal, D. B., V. H. Smith, S. a. J. Declerck, E. C. M. Stam, and J. J. Elser. 2014. Stoichiometric regulation of phytoplankton toxins. Ecol Lett **17:** 736-742.

Vanderploeg, H. A., T. H. Johengen, and J. R. Liebig. 2009. Feedback between zebra mussel selective feeding and algal composition affects mussel condition: did the regime changer pay a price for its success? Freshwater Biol **54:** 47-63.

Vitousek, P.M., and R.W. Howarth. 1991. Nitrogen limitation on land and sea: How can it occur? Biogeochemistry **13**: 87-115.

Wool, T., Davie, S., and Rodriguez, H. 2003. Development of three-dimensional hydrodynamic and water quality models to support total maximum daily load decision process for the Neuse River Estuary, North Carolina. J. Water Resour. Plann. Manage. **129**(4): 295-306.

Yuan, L. L., A. I. Pollard, S. Pather, J. L. Oliver, and L. D'anglada. 2014. Managing microcystin: identifying national-scale thresholds for total nitrogen and chlorophyll a. Freshwater Biol **59:** 1970-1981.

Yuan, Y. and V.E. Johnson. 2012. Goodness of fit diagnostics for Bayesian hierarchical models. Biometrics **68**(1): 156-164.

Table captions

Table 1. Summary of sample size for study sites

Table 2. Geomorphological typology of Finnish lakes specified by Finnish Environmental Institute (SA=surface area, d=depth)

Table 3. The prior distribution for hyper-parameters

Table 1.

					Groups					
Finnish lakes	I	II	III	IV	V	VI	VII	VIII	IX	
	485	6536	388	3949	1080	1326	391	2729	2544	
Saginaw Bay	Apr	May	Jun	Jul	Aug	Sep	Oct	Nov		
	28	59	61	62	49	27	49	44		
Neuse Estuary	Winter					Spring				
	Section1	Section2	Section3	Section4	Section5	Section1	Section2	Section3	Section4	Section5
	137	137	174	131	170	154	146	170	125	158
	Summer					Fall				
	Section1	Section2	Section3	Section4	Section5	Section1	Section2	Section3	Section4	Section5
	156	147	184	124	136	162	162	218	159	225

Table 2.

Lake Type	Name	Characteristics
I	Large, non-humic	SA>4,000ha, color<30
II	Large, humic	SA>4,000ha, color>30
III	Medium and small, non-humic	SA: 50-4,000 ha, color<30
IV	Medium, humic, and deep	SA: 500-4,000, color: 30-90, d>3m
V	Small, humic, and deep	SA: 50-500 ha, color: 30-90, d>3m
VI	Deep, very humic	Color>90, d>3m
VII	Shallow, non-humic	Color<30, d<3m
VIII	Shallow, humic	Color: 30-90, d<3m
IX	Shallow, very humic	Color>90, d<3m

Table 3.

Parameter	Distribution
σ_{N_j}	Uniform [0,4]
σ_{P_j}	Uniform [0,4]
ρ	Uniform [-1,1]
μ_N	Normal $(0,100^2)$
μ_P	Normal $(0,100^2)$
τ_N	Uniform [0,4]
τ_P	Uniform [0,4]
φ	Uniform [-1,1]

Figure captions

Figure 1. (a) Finnish lakes, (b) Saginaw Bay, Lake Huron Michigan, (c) Neuse Estuary, North Carolina; also showing the monitoring stations (black circle) with respect to the five estuarine sections of the Neuse, which are delineated with black lines.

Figure 2. Relationships between N (µg/L) and P (µg/L) concentrations for a,d,g) Finnish lakes, b,e,h) Saginaw Bay, and c,f,i) the Neuse Estuary. In panels a-c) color-symbol combinations, marked differently by group, denote individual observations. In panels d-f) ellipses denote the 95% contour of joint distribution of group N and P from the BHBM. In panels g-i) ellipses denote the 95% contour of joint distribution of overall system N and P from the BHBM. In all panels, solid diagonal lines indicate the Redfield ratio (mass N:P=7.2:1). In panels f), abbreviations are the combination of section and season: the number indicates the sections 1-5 and the text indicates the season (W: Winter, Sp: Spring, Su: Summer, and F: Fall).

Figure 3. Across-group (φ) and within-group (ρ) correlation between N and P for a) Finnish lakes and b) Saginaw Bay, and c) the Neuse Estuary. Gray symbol and gray vertical line denote the mean and 95% interval estimated using the Bayesian hierarchical model.

Figure 4. Group N:P distribution for a) Finnish lakes, b) Saginaw Bay, and c) Neuse Estuary. Gray circle and gray vertical line denote the median and 95% interval estimated using the Bayesian hierarchical model. Solid horizontal line indicates the Redfield ratio (mass N:P=7.2:1).

Figure 1.

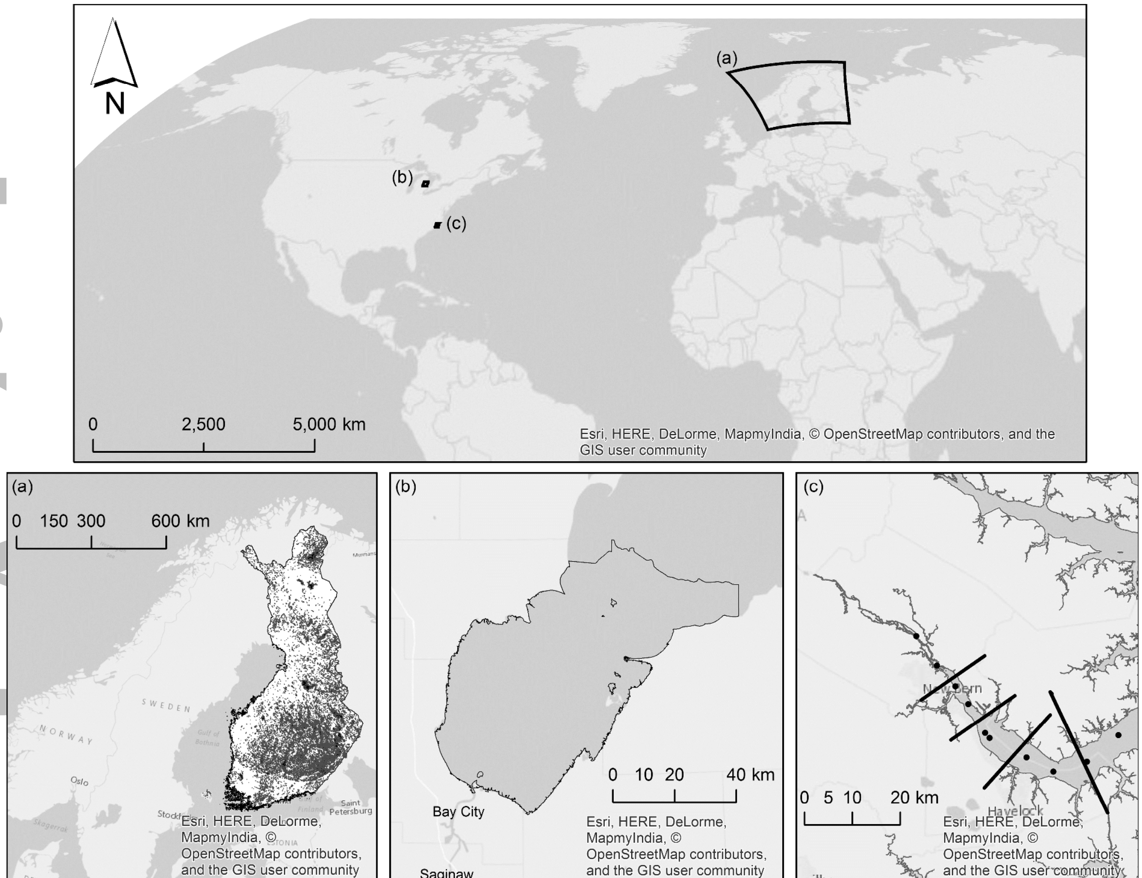
N
(a)
(b)
(c)
0
2,500
5,000 km
Esri, HERE, DeLorme, MapmyIndia, © OpenStreetMap contributors, and the GIS user community
(a)
0 150 300 600 km
SWEDEN
NORWAY
Oslo
Esri, HERE, DeLorme, MapmyIndia, © OpenStreetMap contributors, and the GIS user community
(b)
0 10 20 40 km
Bay City
Saginaw
Esri, HERE, DeLorme, MapmyIndia, © OpenStreetMap contributors, and the GIS user community
(c)
0 5 10 20 km
Havelock
Esri, HERE, DeLorme, MapmyIndia, © OpenStreetMap contributors, and the GIS user community

Figure 2.

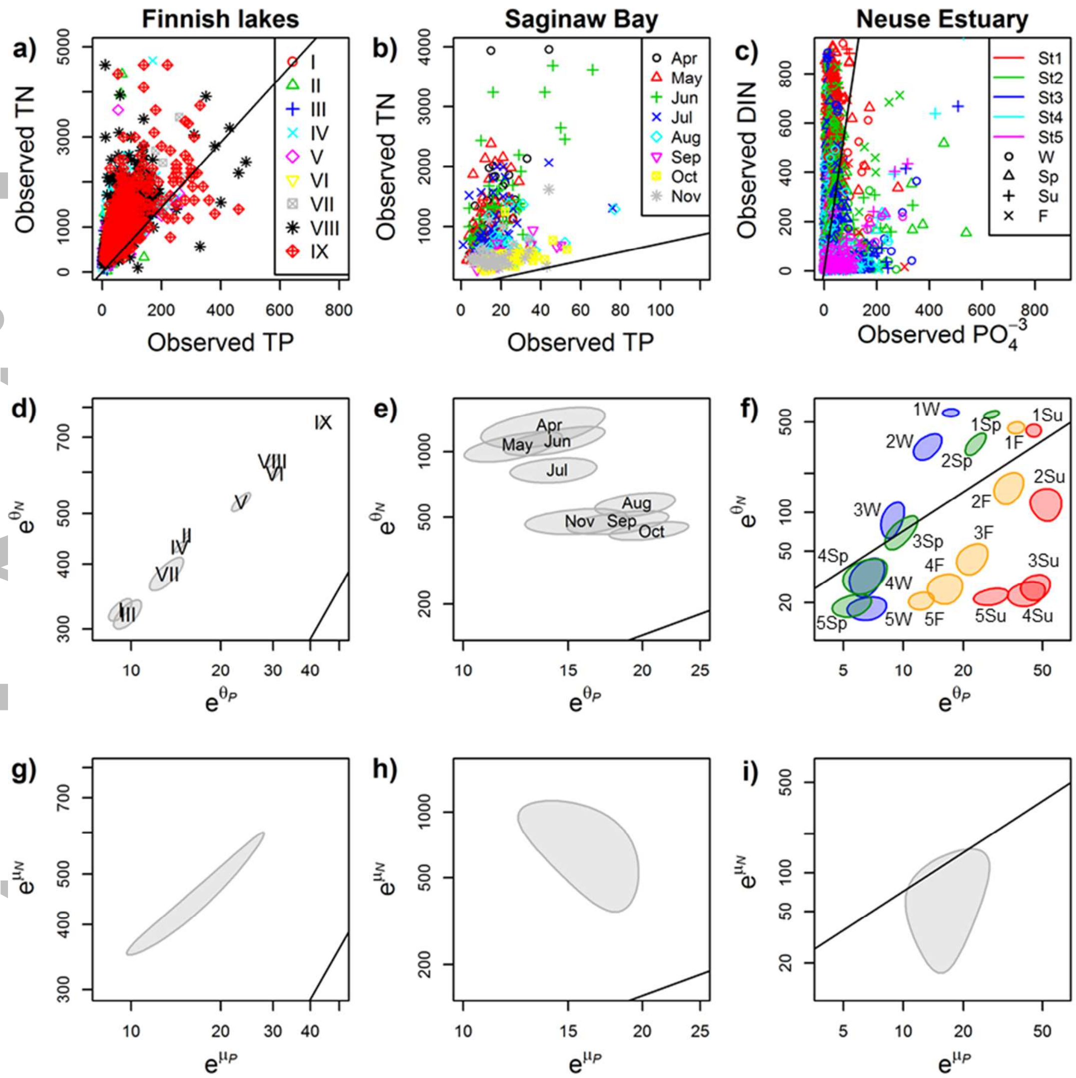
Finnish lakes
Saginaw Bay
Neuse Estuary
a)
b)
c)
Observed TN
Observed TP
Observed DIN
Observed PO_4^{-3}
I
II
III
IV
V
VI
VII
VIII
IX
Apr
May
Jun
Jul
Aug
Sep
Oct
Nov
St1
St2
St3
St4
St5
W
Sp
Su
F
d)
e)
f)
e^{θ_N}
e^{θ_P}
1W
1Sp
1Su
1F
2W
2Sp
2Su
2F
3W
3Sp
3F
3Su
4Sp
4W
4F
5Sp
5W
5F
5Su
4Su
g)
h)
i)
e^{μ_N}
e^{μ_P}

Figure 3.

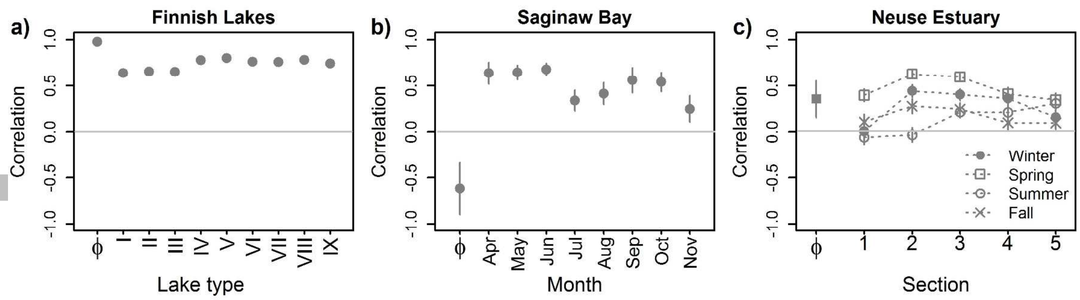
a)
Finnish Lakes
Correlation
1.0
0.5
0.0
-0.5
-1.0
ϕ
I
II
III
IV
V
VI
VII
VIII
IX
Lake type
b)
Saginaw Bay
Correlation
ϕ
Apr
May
Jun
Jul
Aug
Sep
Oct
Nov
Month
c)
Neuse Estuary
Correlation
Winter
Spring
Summer
Fall
ϕ
1
2
3
4
5
Section

Figure 4.

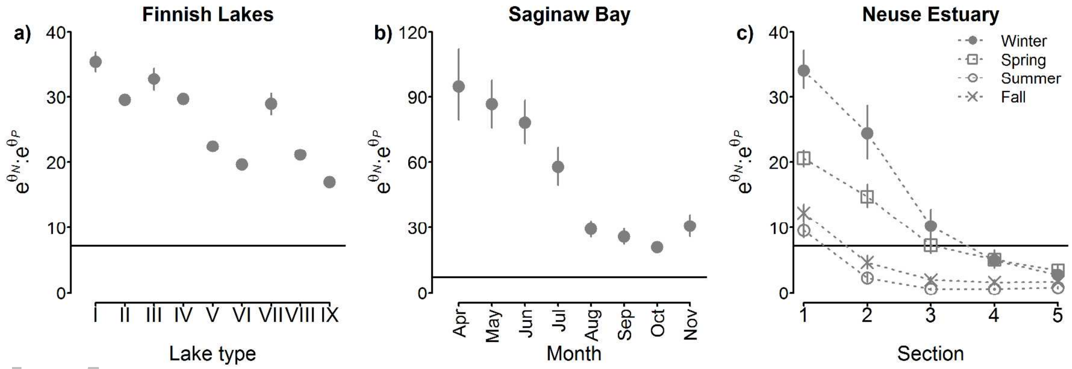
a)
Finnish Lakes
b)
Saginaw Bay
c)
Neuse Estuary
Winter
Spring
Summer
Fall
Lake type
Month
Section
Apr
May
Jun
Jul
Aug
Sep
Oct
Nov
I
II
III
IV
V
VI
VII
VIII
IX

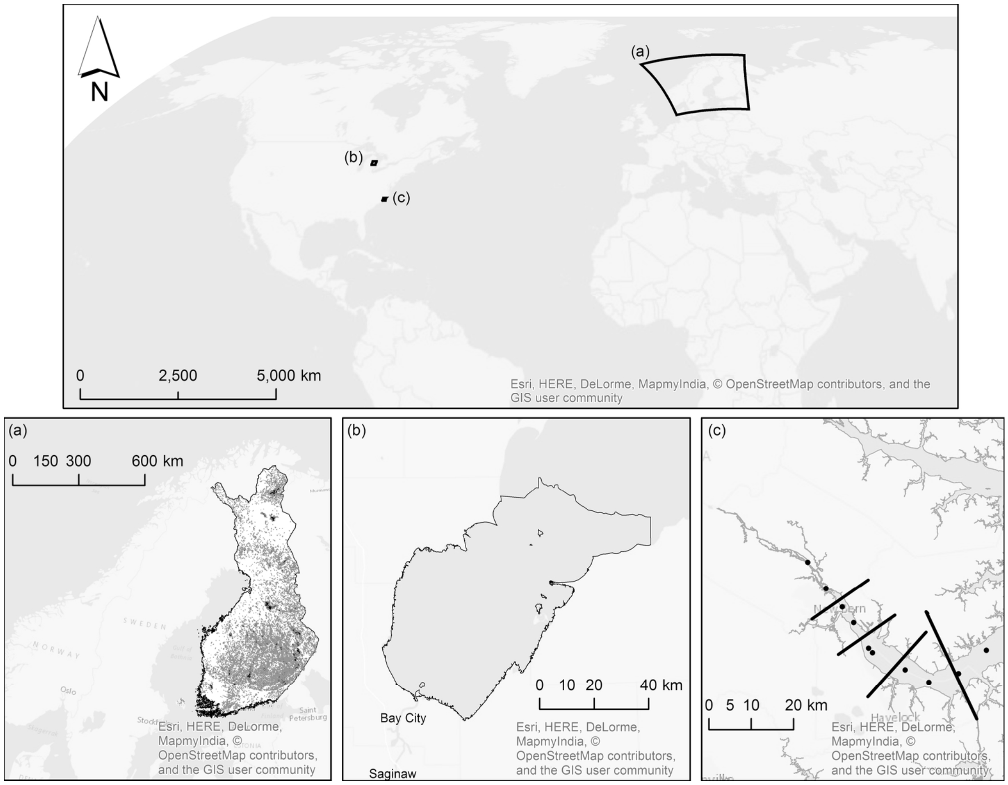

Figure 1. (a) Finnish lakes, (b) Saginaw Bay, Lake Huron Michigan, (c) Neuse Estuary, North Carolina; also showing the monitoring stations (black circle) with respect to the five estuarine sections of the Neuse, which are delineated with black lines.
176x136mm (300 x 300 DPI)

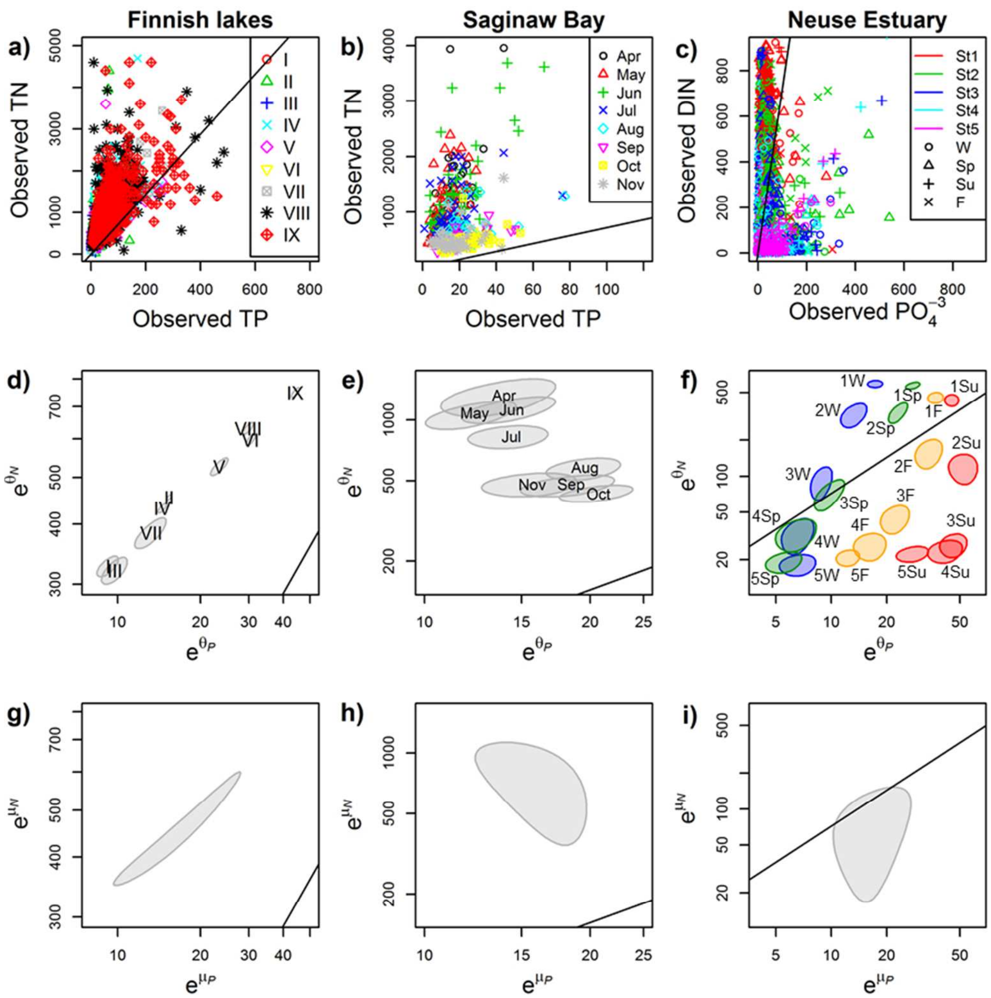

Figure 2. Relationships between N (μg/L) and P (μg/L) concentrations for a,d,g) Finnish lakes, b,e,h) Saginaw Bay, and c,f,i) the Neuse Estuary. In panels a-c) color-symbol combinations, marked differently by group, denote individual observations. In panels d-f) ellipses denote the 95% contour of joint distribution of group N and P from the BHBM. In panels g-i) ellipses denote the 95% contour of joint distribution of overall system N and P from the BHBM. In all panels, solid diagonal lines indicate the Redfield ratio (mass N:P=7.2:1). In panels f), abbreviations are the combination of section and season: the number indicates the sections 1-5 and the text indicates the season (W: Winter, Sp: Spring, Su: Summer, and F: Fall).

152x152mm (150 x 150 DPI)

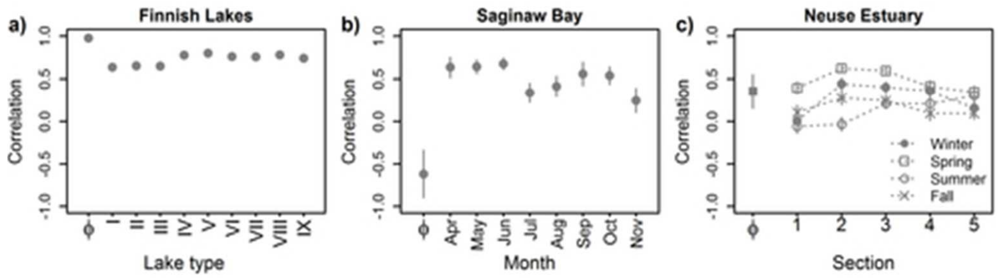

Figure 3. Across-group (φ) and within-group (ρ) correlation between N and P for a) Finnish lakes and b) Saginaw Bay, and c) the Neuse Estuary. Gray symbol and gray vertical line denote the mean and 95% interval estimated using the Bayesian hierarchical model.
42x11mm (300 x 300 DPI)

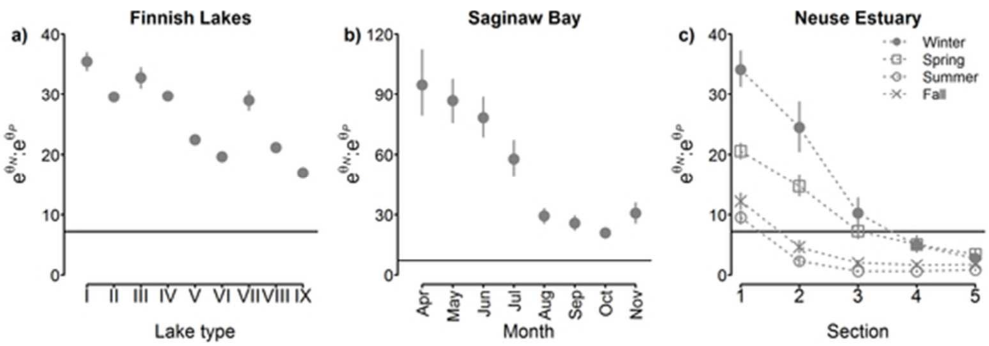

Figure 4. Group N:P distribution for a) Finnish lakes, b) Saginaw Bay, and c) Neuse Estuary. Gray circle and gray vertical line denote the median and 95% interval estimated using the Bayesian hierarchical model. Solid horizontal line indicates the Redfield ratio (mass N:P=7.2:1).
50x16mm (300 x 300 DPI)

Finnish Lakes WinBUGS code[1]:

```
model{
	for (i in 1:n){ #n is the total number of samples collected across all lakes
		y[i,1:2]~dmnorm(y.hat[i,1:2],tau.y[K[i],1:2,1:2]) #bivariate normal distribution for the log N and
								log P measured concentrations by lake type
			y.hat[i,1]<-lamb.space[K[i],1]
			y.hat[i,2]<-lamb.space[K[i],2]
	}
mean.finnish[1]<-mean(lamb.space[,1]) #Overall mean of log N for the Finnish Lakes
mean.finnish[2]<-mean(lamb.space[,2]) #Overall mean of log P for the Finnish Lakes

#Lake type
	for (s in 1:9){ #s is the number of lake types. Check Table 1 in the manuscript & Qian book page 381
		lamb.space[s,1:2]~dmnorm(mu[1:2], tau.lamb[1:2,1:2]) # system-level bivariate normal
								distribution for log N & log P across lake
								types
		sigma.y1[s]~dunif(0,4) #Vague priors on the standard deviations assigned to log N per lake type
		sigma.y2[s]~dunif(0,4) #Vague priors on the standard deviations assigned to log P per lake type
		rho[s]~dunif(-1,1) #Vague priors assigned to the correlation between log N and log P per lake type
		tau.y[s,1:2,1:2]<-inverse(Sigma.y[s,1:2,1:2]) #Building the precision  matrices
		Sigma.y[s,1,1]<-pow(sigma.y1[s],2)
		Sigma.y[s,2,2]<-pow(sigma.y2[s],2)
		Sigma.y[s,1,2]<-rho[s]*sigma.y1[s]*sigma.y2[s]
		Sigma.y[s,2,1]<-Sigma.y[s,1,2]

		for(j in 1:2){
			delta.f[s,j]<-lamb.space[s,j]-mean.finnish[j]
			}
		}
	mu[1]~dnorm(0,0.01) # Vague prior on the overall mean of the system-wide log N concentration
	mu[2]~dnorm(0,0.01) # Vague prior on the overall mean of the system-wide log N concentration

	tau.lamb[1:2,1:2]<-inverse(sigma.lamb[,] )# Building the precision  matrix for the system-wide bivariate
							distribution
	sigma.lamb[1,1]<-pow(sigma.lamb1,2)
	sigma.lamb1~dunif(0,4) #Vague prior
	sigma.lamb[2,2]<-pow(sigma.lamb2,2)
	sigma.lamb2~dunif(0,4) #Vague prior
	sigma.lamb[1,2]<-rho.h*sigma.lamb1*sigma.lamb2
	sigma.lamb[2,1]<-sigma.lamb[1,2]
	rho.h~dunif(-1,1) #Vague prior
}
```

Saginaw Bay WinBUGS code:

```
model{
	for (i in 1:n){ #n is the total number of samples collected across all lakes
		y[i,1:2]~dmnorm(y.hat[i,1:2],tau.y[J[i],1:2,1:2]) #bivariate normal distributions for the log N and
								log P measured concentrations by month
		y.hat[i,1]<-lamb.month[J[i],1]
		y.hat[i,2]<-lamb.month[J[i],2]
}
```

[1] Winbugs automatically comments out all text following the # on a given line. As such, all text following the # is not part of the Winbugs code. It is added to provide an explanation to the adopted model structures.

```
mean.sag[1]<-mean(lamb.month[,1]) #Overall mean of log N for the Saginaw Bay
mean.sag[2]<-mean(lamb.month[,2])  #Overall mean of log P for the Saginaw Bay


        for (m in 1:8){ # m is index for month; April is month 1 (April is m=1)
                lamb.month[m,1:2]~dmnorm(mu[1:2], tau.lamb[1:2,1:2]) # system-level bivariate normal
                                                                        distribution for log N & log P across all
                                                                        months
                sigma.y1[m]~dunif(0,5000) #Vague priors on the standard deviations assigned to log N by month
                sigma.y2[m]~dunif(0,100) #Vague priors on the standard deviations assigned to log P by month
                rho[m]~dunif(-1,1) ) #Vague priors assigned to the correlation between log N & log P by month
                tau.y[m,1:2,1:2]<-inverse(Sigma.y[m,1:2,1:2]) #Building the precision  matrices
                Sigma.y[m,1,1]<-pow(sigma.y1[m],2)
                Sigma.y[m,2,2]<-pow(sigma.y2[m],2)
                Sigma.y[m,1,2]<-rho[m]*sigma.y1[m]*sigma.y2[m]
                Sigma.y[m,2,1]<-Sigma.y[m,1,2]
                for(j in 1:2){
                        delta.m[m,j]<-lamb.month[m,j]-mean.sag[j]
                }
        }
        mu[1]~dnorm(0,0.001) # Vague prior on the overall mean of the system-wide log N concentration
        mu[2]~dnorm(0,0.001) # Vague prior on the overall mean of the system-wide log N concentration
        tau.lamb[1:2,1:2]<-inverse(sigma.lamb[,]) # Building the precision  matrix for the system-wide bivariate
                                                        distribution
        sigma.lamb[1,1]<-pow(sigma.lamb1,2)
        sigma.lamb1~dunif(0,1000) #Vague prior
        sigma.lamb[2,2]<-pow(sigma.lamb2,2)
        sigma.lamb2~dunif(0,100) #Vague prior
        sigma.lamb[1,2]<-rho.h*sigma.lamb1*sigma.lamb2
        sigma.lamb[2,1]<-sigma.lamb[1,2]
        rho.h~dunif(-1,1) #Vague prior
}
```

Neuse Estuary WinBUGS code:

```
model
{
        for (i in 1:n){ #n is the total number of samples collected in the Neuse
                y[i,1:2]~dmnorm(y.hat[i,1:2],tau.y[U[i],1:2,1:2]) #bivariate normal distributions for the log N and
                                                                        log P measured concentrations by section
                                                                        and over season
                for (j in 1:2){
                        y.hat[i,j]<- season.section[U[i],j]
                }
                        }
        mean.modmon[1]<- mean(season.section[,1]) #Overall mean of log N for the Neuse
        mean.modmon[2]<- mean(season.section[,2]) #Overall mean of log P for the Neuse

        for (u in 1:20){ # 20 is the number of section-month combinations in the Neuse; 5 sections and 4 seasons
                season.section[u,1:2]~dmnorm(mu[1:2], tau.lamb[1:2,1:2]) # system-level bivariate normal
                                                                        distribution for log N & log P across all
                                                                        seasons and sections
                sigma.y1[u]~dunif(0,4) #Vague priors on the standard deviations assigned to log N per section-
                                        season combination
                sigma.y2[u]~dunif(0,4) #Vague priors on the standard deviations assigned to log P per section-
                                        season combination
```

```
        rho[u]~dunif(-1,1) #Vague priors assigned to the correlation between log N & log P per section-
                              season combination
        tau.y[u,1:2,1:2]<-inverse(Sigma.y[u,1:2,1:2]) #Building the precision  matrices
        Sigma.y[u,1,1]<-pow(sigma.y1[u],2)
        Sigma.y[u,2,2]<-pow(sigma.y2[u],2)
        Sigma.y[u,1,2]<-rho[u]*sigma.y1[u]*sigma.y2[u]
        Sigma.y[u,2,1]<-Sigma.y[u,1,2]
        for (j in 1:2){
        delta.ss[u,j]<- season.section[u,j] - mean.modmon[j]
                }
        }
    mu[1]~dnorm(0,0.01) ) # Vague prior on the overall mean of the system-wide log N concentration
    mu[2]~dnorm(0,0.01) ) # Vague prior on the overall mean of the system-wide log P concentration
    tau.lamb[1:2,1:2]<-inverse(sigma.lamb[,])# Building the precision  matrix for the system-wide bivariate
                              distribution
    sigma.lamb[1,1]<-pow(sigma.lamb1,2)
    sigma.lamb1~dunif(0,4) #Vague prior
    sigma.lamb[2,2]<-pow(sigma.lamb2,2)
    sigma.lamb2~dunif(0,4) #Vague prior
    sigma.lamb[1,2]<-rho.h*sigma.lamb1*sigma.lamb2
    sigma.lamb[2,1]<-sigma.lamb[1,2]
    rho.h~dunif(-1,1) #Vague prior
}
```